

# Effect of $E/P$ Ratio on the Rheology and Morphology of Crosslinkable Polyethylene and EPDM Blends

P. MUKHOPADHYAY\* and C. K. DAS,  
*Materials Science Center, I.I.T.,  
Kharagpur 721302, India*

## Synopsis

Effects of  $E/P$  ratio of the EPDM rubber on the flow behavior and morphology of the crosslinkable polyethylene and EPDM blends have been studied as a function of shear rate and processing temperature. High- $E/P$ -ratio EPDM rubber exhibits high viscosities within the temperature range studied but the extrudate swell is higher for the low  $E/P$  ratio EPDM. Shear modulus, stored elastic energy and flow activation energy are higher for high  $E/P$  ratio EPDM but relaxation time is higher for low  $E/P$  ratio EPDM. At a particular blend ratio these rheological parameters show a change in their pattern. This point of change in pattern occurs at a lower level of EPDM having a high  $E/P$  ratio; this suggests an early phase inversion as corroborated by the SEM studies. Melt fracture occurs to a larger extent for the low  $E/P$  ratio EPDM in its blends with XLPE.

## INTRODUCTION

Polymer blends are of growing industrial importance. To optimize commercial operations, the rheology of polyblend systems must be known. The blends prepared by melt mixing of a thermoplastic resinous materials and elastomers have gained considerable attention in recent years.<sup>1-5</sup> The incorporation of crosslinking agents improve the mechanical properties of the blends.<sup>6-8</sup> A number of excellent papers concerned with establishing the compatibility or noncompatibility of blends of various elastomers have appeared,<sup>1-10</sup> and it is clear now that nearly all blends are comprised of elastomer domains dispersed in matrices of the other polymers. There is very little published systematic information concerning the flow behavior of elastomer blends. The use of polyethylene in blends and composites is most useful from the technological point of view. For the polymer rheologist it offers a unique opportunity to study the influence of nonchemical effects on rheology and processibility of blends.<sup>11</sup> Utracki et al.<sup>12</sup> studied the flow behavior of various polyethylene blends. He also studied the filler effects on the flow of polyethylene.<sup>13</sup> Illing<sup>14</sup> studied the structure properties of polyblend systems by SEM while Richer<sup>15</sup> studied them by X-ray and TEM analysis. Plochocki<sup>16</sup> investigated the melt elasticity of the LDPE/PP blends using extrudate swell and relaxation spectra. Feng et al.<sup>17</sup> studied the morphology of PP and EPR blends and used EPR as a compatibilizer for PE/PP blends. Recently Das et al.<sup>18-21</sup> studied

\*Department of Chemistry, I.I.T., Kharagpur 721302, India.

rheological behavior of crosslinkable polyethylene with other elastomers with the help of torque rheometry and capillary rheometry.

This paper presents our study on the rheological investigation of crosslinkable polyethylene and EPDM (of different  $E/P$  ratio) blend through characterization of blend morphology. Efforts have been made to detect the effect of  $E/P$  ratio on the blend rheology and morphology of the blends.

### EXPERIMENTAL

Blend compositions were made by gradual replacement of XLPE with EPDM as shown in Table 1. Blending was done in a Brabender plasticorder (PLE-330) at 60 rpm and 120°C for 10 min. An MCR-3210 capillary rheometer along with an Instron-1195 universal testing machine was used to study the melt flow behavior of the blends. The  $L/D$  ratio of the capillary was 40.0. Two types of EPDM rubbers, differing in  $E/P$  ratio, were used in blends with XLPE. They are Intolan-255 ( $E/P = 80/20$ ) and Intolan-155 ( $E/P = 60/40$ ) both from International Synthetic Rubber Co. (U.K.). Five shear rates and three temperatures were selected for the study of rheology. The non-Newtonian index ( $n$ ) and consistency index ( $k$ ) were determined from shear stress and shear rate data by regression analysis.

Activation energy of flow was determined from the change in viscosity with temperature as a function of shear rate as described earlier.<sup>21,22</sup> Extrudate samples were used to determine the swelling ratio ( $\alpha$ ) with the help of a microscope fitted with a micrometer. Viscoelastic parameters like stored elastic energy ( $W$ ), shear modulus ( $G$ ), relaxation time ( $t_R$ ), etc. were determined following the mathematical model as developed by the authors,<sup>21,23</sup> as given below:

$$\gamma_m = \sqrt{(1/2c)(\alpha^4 + 20c^{-2} - 3)}$$

where  $c = (3n + 1)/4(5n + 1)$  and  $\gamma_m$  is recoverable deformation,

$$W = c\gamma_m\tau$$

$$t_R = [1/(\tau^{(1-n)/n})] \cdot [(n \cdot K^{1/n})/G(1-n)] \{ \exp[(1-n)/n] - 1 \}.$$

The morphology of the blends<sup>24-26</sup> was studied with the help of scanning electron microscopy.

TABLE I  
Blend Formulations

Blend nos.	A	B	C	D	E	F	G	A'	B'	C'	D'	E'	F'	G'
Crosslinkable polyethylene (XLPE) <sup>a</sup>	85	70	60	50	40	30	15	85	70	60	50	40	30	15
EPDM-255 <sup>b</sup>	15	30	40	50	60	70	85	—	—	—	—	—	—	—
EPDM-155 <sup>c</sup>	—	—	—	—	—	—	—	15	30	40	50	60	70	85

<sup>a</sup> XLPE-11 - ML<sub>1+4</sub> (120°C) = 18.0, MFI (10 min, 5.0 kg, 140°C) = 2.40, density = 0.915 gm/cc.

<sup>b</sup> Intolan-225 - ML<sub>1+4</sub> (120°C) = 70,  $E/P = 80/20$ .

<sup>c</sup> Intolan-155 - ML<sub>1+4</sub> (120°C) = 68,  $E/P = 60/40$ .

## RESULTS AND DISCUSSION

Effect of Blend Ratio and  $E/P$  Ratio on the Melt Viscosity

Variation of melt viscosity at  $130^{\circ}\text{C}$  as a function of shear rate is represented graphically in Figures 1 and 2 for two types of EPDM. The melt viscosity decreases logarithmically with the shear rate for all the blends. At a particular shear rate the viscosity increases as the XLPE/EPDM ratio decreases. This trend holds true for both the types of EPDM used. Increasing temperature, however, decreases the viscosity of the blends at all shear rates studied, but relative difference in viscosity between the blends diminishes. The straight line plots tend to converge at the high shear rate region. At high temperature these become closer.

Variation of melt viscosity with the blend ratio for both the EPDM rubbers in the blend with XLPE has been shown as a logarithmic plot of viscosity against blend ratio in Figure 3. There are three distinct stages in the change of viscosity with addition of EPDM in XLPE. First there is a rapid rise in viscosity with the initial addition of EPDM, then a slow increase, and lastly a sharp increase in viscosity is observed at the high loading of EPDM in the blend. The trend is the same for both EPDM rubbers at the initial stage comparatively rapid rise is observed with EPDM of high  $E/P$  (80:20) ratio. The onset of the second stage also occur earlier in the case of high  $E/P$  ratio EPDM rubber. However, the third stage show a comparatively sharp trend of

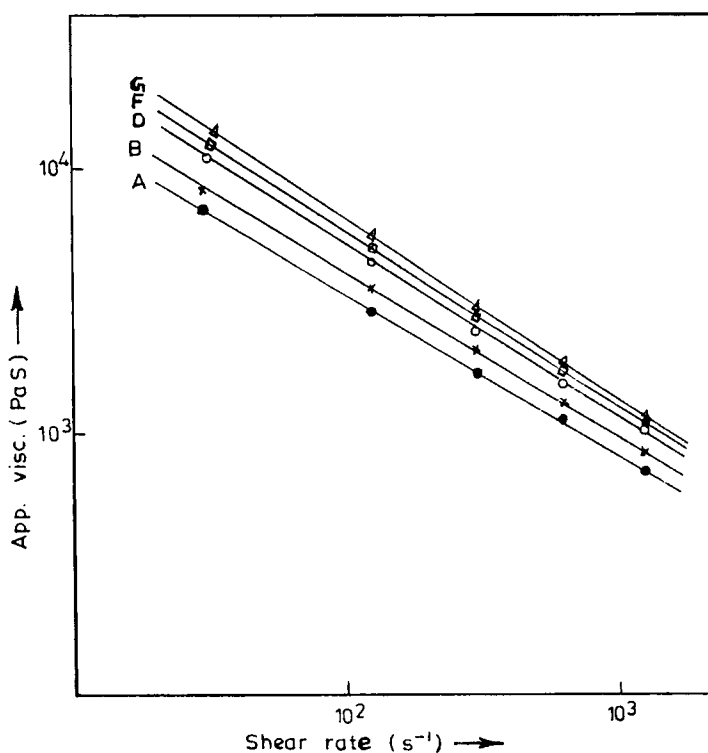


Fig. 1. Variation of apparent viscosity with shear rate for the blends at  $130^{\circ}\text{C}$ .

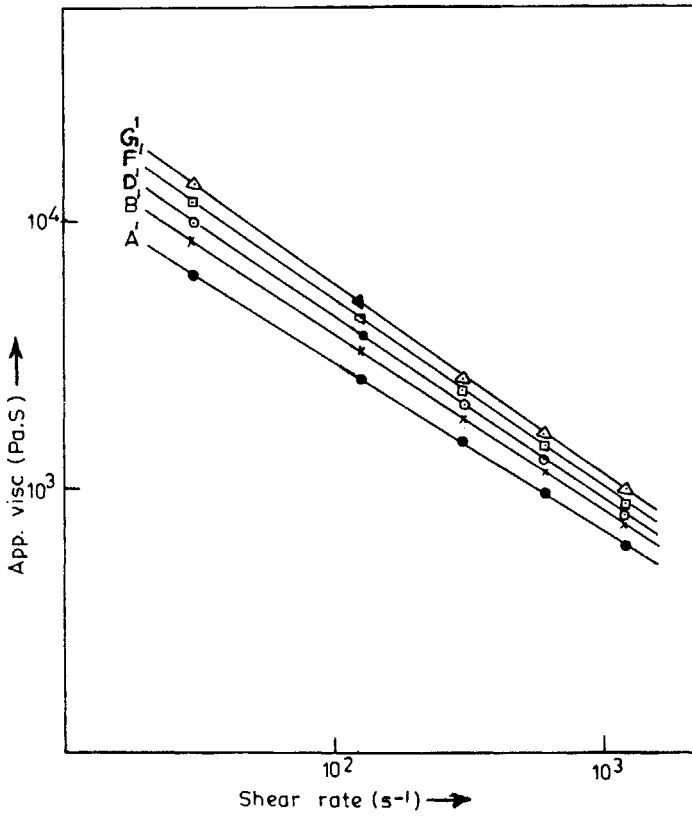


Fig. 2. Variation of apparent viscosity with shear rate for the blends at 130°C.

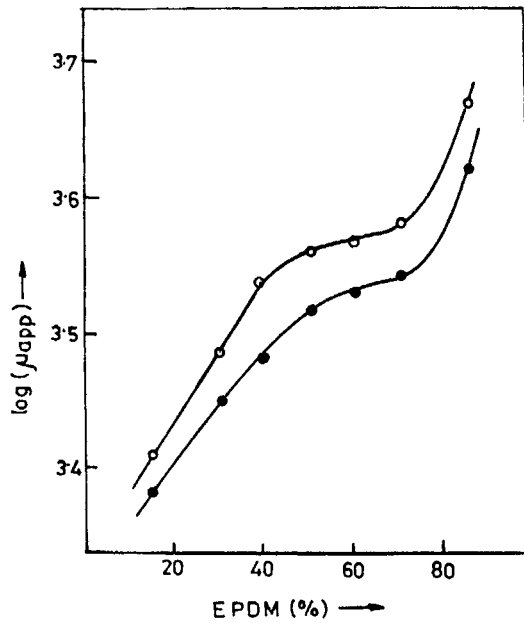


Fig. 3. Variation of viscosity (at 140°C, 100 s<sup>-1</sup>) with blend ratio [*E*:*P* = 80:20 (○); *E*:*P* = 60:40 (●)].

increasing viscosity with the low  $E/P$  (60 : 40) ratio EPDM rubber. At higher temperature the nature of the plot remains unaltered, only the difference between the two plots narrows down and at very high EPDM/XLPE level the 60 : 40  $E/P$  ratio EPDM shows slightly higher viscosity than 80 : 20  $E/P$  ratio EPDM.

### Effect of Blend Ratio and $E/P$ Ratio on the Power Law Indices

The non-Newtonian index  $n$  as determined by regression analysis is plotted against the blend ratio in Figure 4 for both blends. As observed  $n$  decreases as the XLPE/EPDM ratio decreases, but the rate of decrease depends on the  $E/P$  ratio of the EPDM added. A rapid decrease is observed for the EPDM having 60 : 40  $E/P$  ratio. The plot shows two distinct stages, a rapid decrease in  $n$  values followed by a slow decreasing stage. The transition between these two stages occurs at a higher XLPE/EPDM level for EPDM having an 80 : 20  $E/P$  ratio than with EPDM having a 60 : 40  $E/P$  ratio. This trend is maintained for all the temperatures of processing studied. An increase in processing temperature increases the non-Newtonian index for all the blend

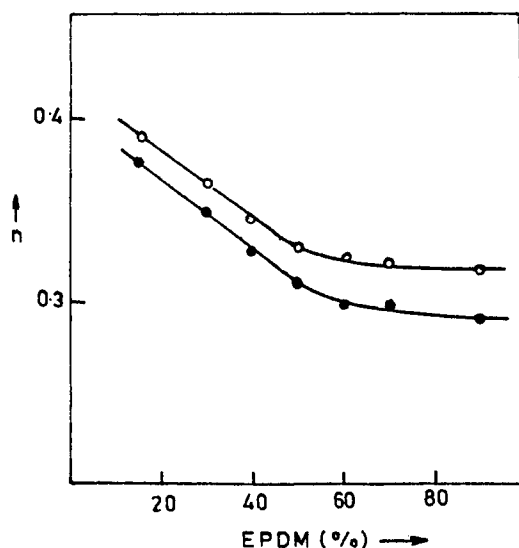


Fig. 4. Variation of non-Newtonian index ( $n$ ) with blend ratio [ $E : P = 80 : 20$  (○);  $E : P = 60 : 40$  (●)] at 130°C.

TABLE II  
Values of Consistency Index ( $K$ ) at 130°C

Blend nos.	$K \times 10^{-4}$	Blend nos.	$K \times 10^{-4}$
A	5.75	A'	5.25
B	7.74	B'	7.76
C	9.41	C'	9.62
D	11.30	D'	11.60
E	11.80	E'	12.50
F	12.10	F'	13.20
G	15.60	G'	15.10

systems. The consistency index ( $K$ ) increases as the XLPE/EPDM ratio decreases (Table II).  $K$  values are found to be higher for the EPDM having lower  $E/P$  (60:40) ratio in the blend. However, increase in temperature decreases the consistency index ( $K$ ).

### Effect of Blend Ratio and $E/P$ Ratio on the Swelling Ratio

A representative example of the extrudate swell behavior has been shown in Figure 5 as a function of shear rate for both the EPDM rubbers in the blend with XLPE. Swelling ratio increases with the shear rate slowly at the low shear rate region and comparatively faster at the high shear rate region. Increase in EPDM content increases the swelling ratio but at the high shear rate region there is rapid rise in swelling for the blends having higher EPDM content. EPDM with low  $E/P$  (60:40) ratio exhibit higher swelling than the EPDM with high  $E/P$  ratio. The above pattern of swelling (Fig. 5) behavior with shear rate is unaffected by the  $E/P$  ratio of EPDM in the blend. Increasing the processing temperature slightly decreased the extrudate swell and the difference due to the  $E/P$  ratio narrowed down.

### Effect of Blend Ratio and $E/P$ Ratio on Rheological Parameters

Rheological parameters like relaxation time, shear modulus, and stored elastic energy are determined following a theoretical model from the extrudate, swell and stress-strain data as described earlier.<sup>23</sup> Representative examples of the variation of these parameters with blend ratio for both the EPDM rubbers were shown in Figures 6, 7, and 8, respectively. Figure 6 depicts that the relaxation time increases sharply with the increase in EPDM/XLPE ratio, although there is a change in pattern at around 50:50 blend ratio level. EPDM with lower  $E/P$  ratio (60:40) in the blend exhibit higher relaxation time than the higher  $E/P$  ratio (80:20) EPDM.  $t_R$  decreases with increasing shear rate. Increase in temperature is associated with decrease of the relaxation time.

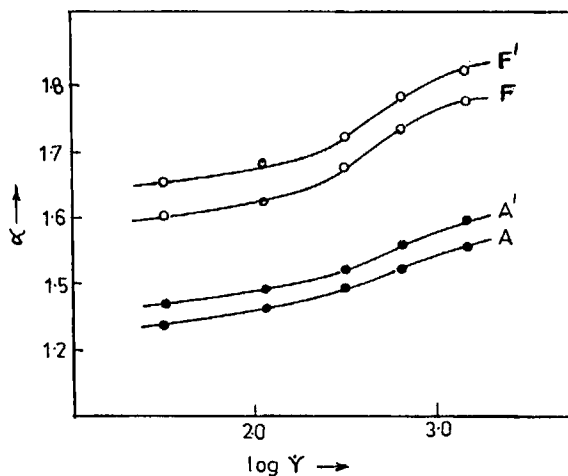


Fig. 5. Variation of extrudate swell (at 130°C) with shear rate for the blends.

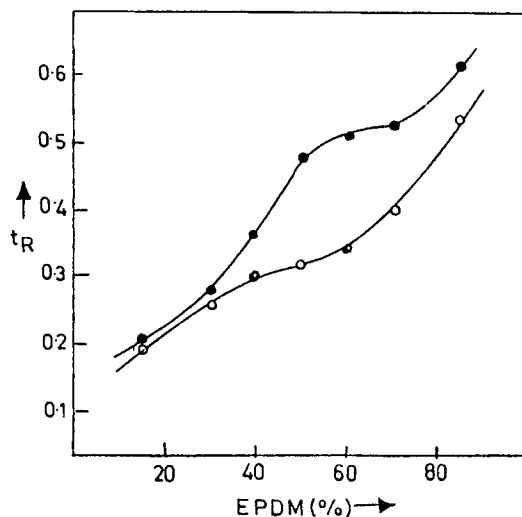


Fig. 6. Variation of relaxation time (at  $130^\circ\text{C}$ ,  $30.585\text{ s}^{-1}$ ) with blend ratio [ $E:P = 80:20$  (○);  $E:P = 60:40$  (●)].

Shear modulus (Fig. 7) increases with the increase in EPDM content in the blend, rapidly at the initial stage but comparatively slowly at the high level of EPDM. Higher  $E/P$  ratio EPDMs show higher shear modulus. Shear modulus increases with increasing shear rate but decrease with increase in extrusion temperature. Stored elastic energy also increases with increase in EPDM content in the blend (Fig. 8) with higher increasing effect for high  $E/P$  ratio EPDM rubber. A change in the pattern is also observed at around 50:50 blend ratio. Shear rate increases the stored elastic energy. Increased extrusion temperature, however, decreases the elastic energy of the blends.

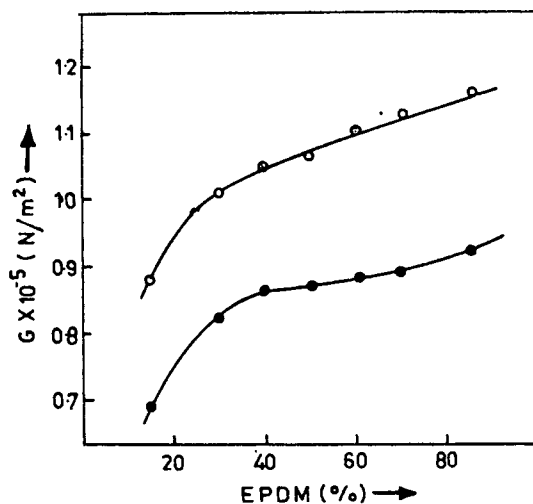


Fig. 7. Variation of shear modulus (at  $130^\circ\text{C}$ ,  $30.585\text{ s}^{-1}$ ) with blend ratio [ $E:P = 80:20$  (○);  $E:P = 60:40$  (●)].

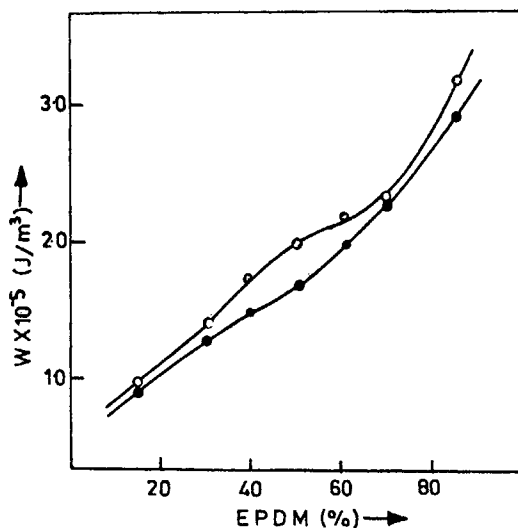


Fig. 8. Variation of stored elastic energy (at  $130^{\circ}\text{C}$ ,  $30.585\text{ s}^{-1}$ ) with blend ratio [ $E : P = 80 : 20$  (○);  $E : P = 60 : 40$  (●)].

### Effect of Blend Ratio and $E/P$ Ratio on Flow Activation Energy

A representative example of variation of viscosity with temperature of processing is shown in Figure 9 at a particular shear rate. A linear relationship confirms the Arrhenius type of behavior from which the flow activation energy can be calculated (Table III) at different shear rates. Increase in shear rate decreases the flow of activation energy, although this decrease is not so well marked at the high shear rate region. This trend is irrespective of the  $E/P$  ratio of the EPDM used in the blend. The variation of flow activation energy is plotted against composition as a function of  $E/P$  ratio of EPDM in

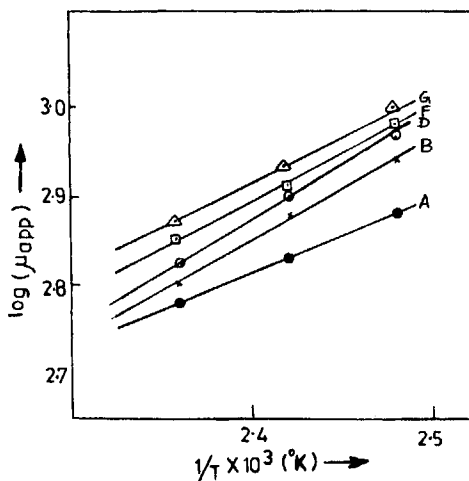


Fig. 9. Variation of viscosity (at  $1223\text{ s}^{-1}$ ) with temperature for blends of EPDM [ $E : P = 80 : 20$ ].



TABLE III  
Flow Activation Energy of the Blends at  $1223 \text{ (s}^{-1}\text{)}$

Blend nos.	$\Delta E$ (kJ/mol)	Blend nos.	$\Delta E$ (kJ/mol)
A	16.4	A'	15.9
B	22.1	B'	21.0
C	19.5	C'	22.0
D	23.1	D'	22.3
E	22.7	E'	21.8
F	22.0	F'	20.9
G	21.2	G'	19.8

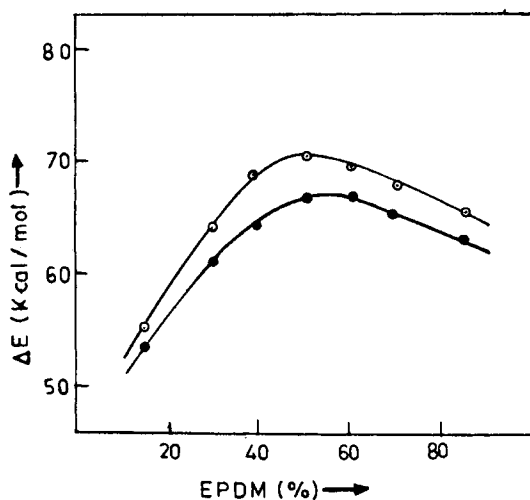


Fig. 10. Variation of flow activation energy (at  $611 \text{ s}^{-1}$ ) with blend ratio [ $E:P = 80:20$  (○);  $E:P = 60:40$  (●)].

Figure 10. As observed, the flow activation energy increases rapidly as the EPDM/XLPE ratio increases, attains a maximum, and then slowly decreases for both the EPDM rubbers used. However, the position of maximum activation energy varies on the blend ratio axis, depending on the  $E/P$  ratio of the EPDM used in the blend. With the EPDM of high  $E/P$  ratio (80:20) the point of maximum flow activation energy occurred at low EPDM/XLPE blend ratio, i.e., at lower percentage of EPDM in the blend. However, with low  $E/P$  ratio (60:40) EPDM, the maximum activation energy point shifts towards higher EPDM percentage side as observed in Figure 10, i.e., as the  $E/P$  ratio decreases, the point of inversion shifts towards higher EPDM dosage in the blend with XLPE. EPDM having higher  $E/P$  ratio exhibits higher activation energy of flow at all the shear rate regions studied.

### SEM Studies on the Morphology of the Blends

SEM photomicrographs of the fracture surface are shown in the Figures 11–18 for both the molded and the extrudate samples. Figures 11–14 show the effect of XLPE/EPDM ( $E/P = 80:20$ ) ratio on the blend morphology. For



Fig. 11. SEM photograph of blend (A) at  $310\times$ .



Fig. 12. SEM photograph of blend (B) at  $310\times$ .

the blend with higher XLPE/EPDM (85/15) ratio the mixing seems to be inhomogeneous (Fig. 11). The minor highly viscous component (EPDM) forms a distinct phase dispersed in the continuous phase of XLPE. However, at the higher level (Fig. 12), the EPDM remains as a dispersed phase in the XLPE continuous phase both as droplets and rodlike structures. At the 50 : 50 blend ratio (Fig. 13) both the components seem to be in continuous phase. At the



Fig. 13. SEM photograph of blend (D) at  $310\times$ .

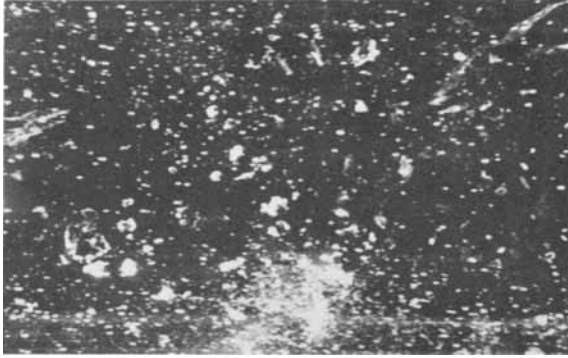


Fig. 14. SEM photograph of blend (F) at  $310\times$ .

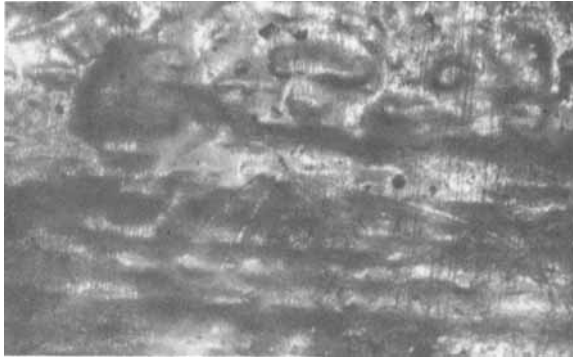


Fig. 15. SEM photograph of blend (B') at  $310\times$ .

still higher level of EPDM (Fig. 14), the EPDMs constitute the continuous phase and XLPE the dispersed phase. As observed, EPDM dispersed in XLPE is much coarser than vice versa i.e., EPDM has larger dimension in XLPE than the XLPE in EPDM.

The effects of  $E/P$  ratio on the morphology are shown in Figures 15 and 16, having the same blend ratio as in Figures 12 and 14, respectively. As the  $E/P$



Fig. 16. SEM photograph of blend (F') at  $310\times$ .

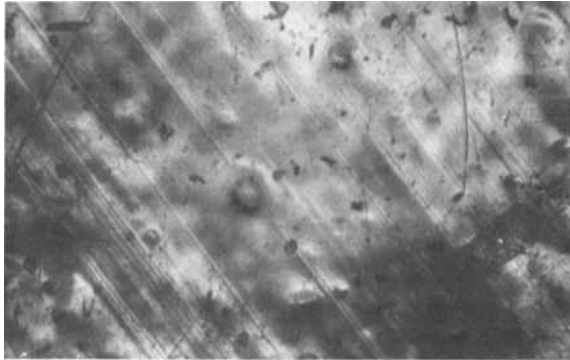


Fig. 17. SEM photograph of extrudate of blend (B) at  $500\times$ .



Fig. 18. SEM photograph of extrudate of blend (B') at  $500\times$ .

ratio of EPDM is decreased (60:40), the dispersion of EPDM in XLPE becomes coarser and prefers to remain mostly in irregular shape. Here again at the higher EPDM level the XLPE remains in the dispersed phase (Fig. 16) but the dispersion becomes coarser than in the EPDM  $E/P$  ratio of 80:20 (Fig. 14).

SEM photomicrographs of the longitudinal cross sections are shown in Figures 17 and 18 for the two types of EPDM at the same blend ratio. The specimens were extruded at  $140^\circ\text{C}$  and at shear rate  $305.85\text{ s}^{-1}$ . Apparently smooth extrudates are observed, but, as observed from the micrographs, the smoother extrudates are formed with smaller droplets EPDM with high  $E/P$  ratio. However, with low  $E/P$  ratio EPDM, both thin fibrils and dispersed droplets are observed.

### Melt Fracture Studies of the Extrudates

The extrudates are shown in Figure 19 as a function of temperature and shear rate. As observed, smooth extrudate is formed at lower level of EPDM (extrudate 1) at low shear rate. At high shear rate the circular ridges with slight tearing on the surface occurred (extrudate 2). As the EPDM content increases, surface irregularities start and shark skin behavior is observed at

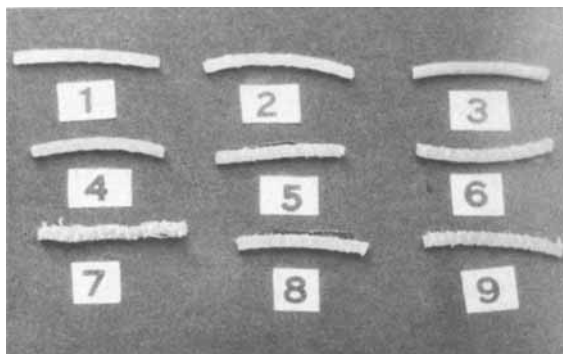


Fig. 19. Photograph of the extrudates: (1) blend A at  $130^{\circ}\text{C}$  and  $30.585\text{ s}^{-1}$ ; (2) blend A at  $130^{\circ}\text{C}$  and  $1223\text{ s}^{-1}$ ; (3) blend F at  $130^{\circ}\text{C}$  and  $30.585\text{ s}^{-1}$ ; (4) blend F at  $130^{\circ}\text{C}$  and  $611.7\text{ s}^{-1}$ ; (5) blend F at  $130^{\circ}\text{C}$  and  $1223\text{ s}^{-1}$ ; (6) blend F' at  $130^{\circ}\text{C}$  and  $611.7\text{ s}^{-1}$ ; (7) blend F' at  $130^{\circ}\text{C}$  and  $1223\text{ s}^{-1}$ ; (8) blend F' at  $140^{\circ}\text{C}$  and  $611.7\text{ s}^{-1}$ ; (9) Blend F' at  $140^{\circ}\text{C}$  and  $1223\text{ s}^{-1}$ .

high shear rates (extrudates 3, 4, and 5). A notable extent of surface tearing occurs in the case of blends with low  $E/P$  ratio EPDM (extrudates 6 and 7). The increase in extrusion temperature decreases the extent of surface tearing (extrudates 8 and 9), but surface irregularities are still found in the case of low  $E/P$  ratio EPDM in the blend with XLPE. Overall melt fracture is less in high  $E/P$  ratio EPDM compared to low  $E/P$  ratio EPDM in the XLPE/EPDM blends.

As observed from the above studies, all the rheological parameters show a distinguished change in their pattern at a particular blend ratio, i.e., at that point the rate of change with blend ratio alters abruptly. For the EPDM rubber having higher  $E/P$  ratio (80:20), this point on the blend ratio axis exists at the lower level of EPDM approximately around 45% of EPDM (i.e., XLPE:EPDM 55:45) whereas for EPDM with low  $E/P$  ratio (60:40) the point of inflection occurs approximately around 55% EPDM (i.e., XLPE:EPDM 45:55). Hence it may be logical to assume that up to 45% of EPDM ( $E/P = 80:20$ ) and 55% of EPDM ( $E/P = 60:40$ ), XLPE forms the continuous phase and EPDM remains as a dispersed system. Beyond this percentage of EPDM, both phases probably become continuous. At a higher level of EPDM, the XLPE becomes the dispersed phase in the continuous phase of EPDM. These changes in behavior may be due to the higher amount of ethylene in the EPDM in the former blend systems. Melt fracture is observed in the case of low  $E/P$  ratio EPDM rubber associated with high extrudate swell behavior, which may be due to higher elastic response of the low  $E/P$  ratio EPDM rubber. SEM studies reveal that the dispersion of the minor component in continuous major component is always coarser (at either end of the blend ratio) in the case of EPDM having low  $E/P$  ratio, which may account for the higher extent of surface irregularities of the extrudates.

### CONCLUSION

Flow behavior and the morphology of the XLPE/EPDM blends depend on the  $E/P$  ratio of the EPDM used and their relative response towards shear rate and temperature of processing. At high temperature and low shear rate,

they do not differ to an appreciable extent but differ widely in low temperature and high shear rate region. It appears that the phase inversion probably occurs at the early level of EPDM when high  $E/P$  ratio EPDM is used. For low  $E/P$  ratio EPDM rubber the point of inversion occurs at a slightly higher level than 50 : 50 of XLPE/EPDM blend ratio. Die swell and melt fracture are higher and prominent in the case of low  $E/P$  ratio EPDM.

Authors wish to thank Professor S. K. Palit, Head, Department of Chemistry for his constructive criticism and valuable suggestions. Thanks are also due to Professor S. Maiti of Materials Science Centre for the guideline.

### References

1. B. M. Walker, *Handbook of Thermoplastic Elastomers*, Van Nostrand Reinhold, New York, 1979.
2. A. P. Plochocki, *Polymer Blends*, Academic, New York, 1978, Vol. 2, Chap. 21.
3. A. Whelan and K. S. Lee, *Developments in Rubber Technology Thermoplastic Rubbers*, Applied Science, London, 1982.
4. S. Danesi and R. S. Porter, *Polymer*, **19**, 448 (1978).
5. L. F. Ramos-De Valle, *Rubber Chem. Technol.*, **55**, 1341 (1982).
6. D. S. Campbell, D. J. Elliot, and M. A. Wheelans, *NR Technol.*, **9**, 21 (1978).
7. A. Y. Coran and R. P. Patel, *Rubber Chem. Technol.*, **53**, 141 (1980).
8. A. Y. Coran and R. P. Patel, *Rubber Chem. Technol.*, **53**, 781 (1980).
9. K. Min and J. L. White, *Polym. Eng. Sci.*, **24**, 1327 (1984).
10. R. Rizzo and G. Sporado, *Polym. Eng. Sci.*, **24**, 264 (1984).
11. L. A. Utracki, *Proc. IX Int. Congress on Rheology Micro*, 1984, P. 567.
12. L. A. Utracki, C. Farha, and M. M. Dumoulin, *Polym. Eng. Sci.*, **24**, 1319 (1984).
13. L. A. Utracki and J. Lara, *Polym. Compos.*, **5**, 44 (1984).
14. G. Illing, *Prog. Colloid Polym. Sci.*, **72**, 97 (1986).
15. K. P. Richer, K. Meyer, M. Kita, and G. Goldbach, *Prog. Colloid Polym. Sci.*, **72**, 83 (1986).
16. A. P. Plochocki, *Trans. Soc. Rheol.*, **20**(2), 287 (1976).
17. Z. Feng, G. Sun, Y. Yang, B. Zhang, and D. Yang *Polym. Eng. Sci.*, **24**, 612 (1984).
18. C. K. Das and D. Khastagir, *Polym. Mater.*, **2**, 2 (1985).
19. C. K. Das, *Proc. IRC Kyoto, Japan*, Oct. 1985.
20. C. K. Das, *Rubber Rep.*, (May/June), (1986).
21. C. K. Das, *Plast. Rubber Proc.*, **8**, 1 (1987).
22. C. K. Das, D. Sinha, S. Kole, and S. Banerjee *Plast Rubber Proc.*, **5**, 3 (1985).
23. C. K. Das, D. Sinha, S. Kole, and S. Banerjee, *Rheol. Acta*, **5**, 507 (1986).
24. S. Radhakrishnan, *Int. J. Polym. Mater.*, **11**, 281 (1987).
25. M. Malinconico, E. Martuscelli, and M. G. Volpe, *Int. J. Polym. Mater.*, **11**, 295 (1987).
26. M. Malinconico, E. Martuscelli, G. Ragosta, and M. G. Volpe, *Int. J. Polym. Mater.*, **11**, 317 (1987).

Received October 19, 1988

Accepted October 25, 1988